scientific reports

OPEN

Synthesis of new hybrid pyridines catalyzed by Fe₃O₄@SiO₂@ urea-riched ligand/Ch-Cl

Narges Zarei, Mohammad Ali Zolfigol✉, Morteza Torabi & Meysam Yarie✉

Herein, a new heterogeneous catalytic system through modification of urea functionalized magnetic nanoparticles with choline chloride [Fe₃O₄@SiO₂@urea-riched ligand/Ch-Cl] was designed and synthesized. Then, the synthesized Fe₃O₄@SiO₂@urea-riched ligand/Ch-Cl was characterized by using FT-IR spectroscopy, FESEM, TEM, EDS-Mapping, TGA/DTG and VSM techniques. After that, the catalytic usage of Fe₃O₄@SiO₂@urea-riched ligand/Ch-Cl was investigated for the synthesis of hybrid pyridines with sulfonate and/or indole moieties. Delightfully, the outcome was satisfactory and the applied strategy represents several advantages such as short reaction times, convenience of operation and relatively good yields of obtained products. Moreover, the catalytic behavior of several formal homogeneous DESs was investigated for the synthesis of target product. In addition, a cooperative vinylogous anomeric-based oxidation pathway was suggested as rational mechanism for the synthesis of new hybrid pyridines.

Deep eutectic solvents (DESs) as an emerging alternative to ionic liquids and organic solvents have a brilliant breakthrough in many scientific areas[1–4]. Low vapor pressure, tunable physiochemical properties, high polarity, biodegradability, greener and excellent catalytic activity of DESs are usually highlighted[5–8]. Recently, DESs linked to heterogeneous supports, as a new subclass of heterogeneous systems, have a creating and implementing beneficial and neoteric chemical transformations[9–11]. DESs have applied for modification of the surface of some materials such as magnetic nanoparticles (MNPs), metal organic frameworks (MOFs), silicates, covalent organic frameworks (COFs), biopolymers and etc.[12–16]. So, it can be said that these compounds are the forefront of post-synthetic modifications[17]. In this respect, nanomagnetic supported DESs (MDESs) is oriented toward fundamental and synthesis researches. MDESs due to easy reusing and recoverability and workup simplicity create an ingenious insight in many academic and industrial areas[18–21]. These materials have significant potentials and applications in several outlines including solar cells[22], electrochemistry[23], redox flow batteries[24], supercapacitors[25], biosensors[26] and chemical separation processes[27]. Also, due to the simultaneous presence of acidic and basic functional groups and response to external magnetic field, MDESs are a prosperous assortment as sustainable media as well as catalysts in many of organic transformations such as coupling reactions[28–30] and multi-component reactions[31,32]. Recently, there are several studies from catalytic applications of MDESs in multi-component reactions[33–35]. A number of catalytic applications of DESs in multi-component reactions are sketched in below (Fig. 1)[33,36–40].

Despite extensive research on magnetic nanoparticles, these particles are still being researched by scientists due to their unique features and capabilities. These particles have the ability to be a suitable substrate for connecting organic groups. Magnetic nanoparticles have unique properties such as low toxicity, low cost, high magnetic property, compatibility with the environment, high surface area, chemical stability[41–43].

These particles are used as sensors, absorption of organic substances (paints, pharmaceuticals, etc.), water disinfection, wastewater treatment, as well as in the field of biomedicine and cancer treatment[44,45].

Another prominent application of magnetic nanoparticles is their usage as catalysts, which attracted a lot of attention among scientists due to their availability, easy recovery, and reusability[46,47]. Photocatalysis, oxidation/ reduction reactions, multi-component reactions, photoelectrochemical catalysis, coupling reactions and chiral catalysis are examples of catalytic applications of MNPs[48–50]. Therefore, immobilizing catalytically active species on magnetic substrates while maintaining or improving their activity also allows for easy separation. For this reason, these catalytic systems are superior to homogeneous systems.

Molecular hybridization due to its compositional characterization is an interesting structural modification approach which are including of the incorporation of two or more pharmacophores into a single molecule[51,52].

Department of Organic Chemistry, Faculty of Chemistry, Bu-Ali Sina University, Hamedan, Iran. ✉email: mzolfigol@ yahoo.com; myarie.5266@gmail.com
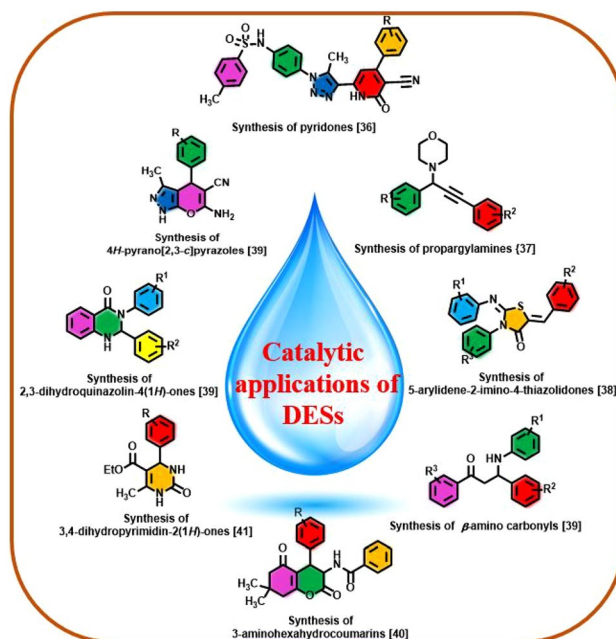
Figure 1. A number of catalytic applications of DESs in multi-component reactions.

The unique performance of hybrid heterocycles is based on the recognition of pharmacophoric moieties in two or more biologically active molecules which preserved or promoted pre-selected properties of the original templates[52,53]. Hybrid pyridines as distinguished scaffolds of heterocyclic compounds not only are extensively present in pharmaceutical active molecules, agricultural compounds and functional materials[54–58] but also are one of the most top-selling drugs and can serve as treatment of Alzheimer's diseases[59], anticancer[60] and antihypertensive[61]. Intriguingly, hybrid molecules bearing pyridine, indole and sulfonate moieties have exceptional potential in pharmaceutical and medicinal chemistry such as antioxidant, antiapoptosis, antidyslipidemia, antitumorigenic, antiinflammatory and can enhance the stability and solubility of drugs[62–67]. A number of biologically active hybrid molecules bearing pyridine, indole and sulfonate moieties are sketched in Fig. 2.
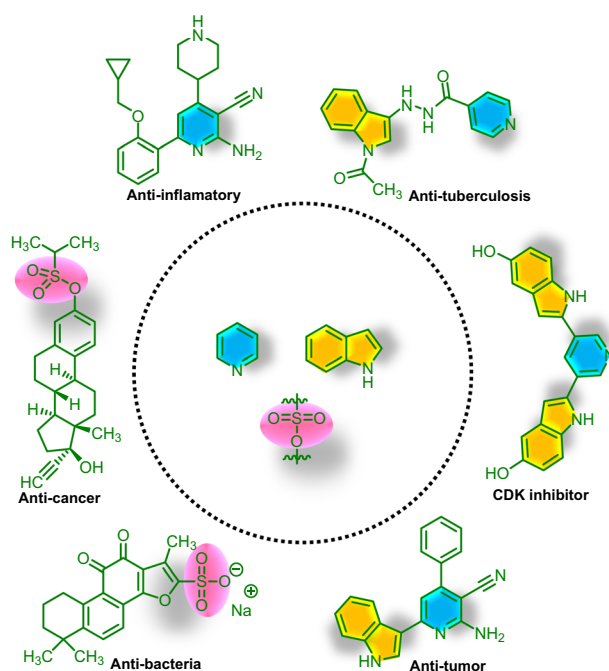

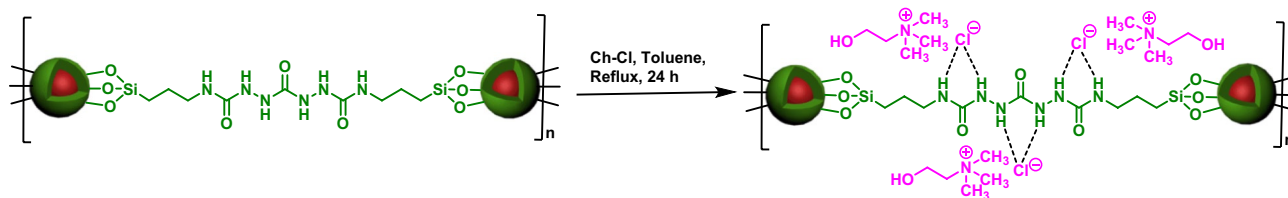**Figure 2.** A number of biologically active hybrid molecules.

Figure 3. General procedure for the synthesis of Fe$_3$O$_4$@SiO$_2$@urea-riched ligand/Ch-Cl.

In this investigation, after synthesis of Fe$_3$O$_4$@SiO$_2$@urea-riched ligand/Ch-Cl, pyridines with indole and/or sulfonate moieties were synthesized in the presence of Fe$_3$O$_4$@SiO$_2$@urea-riched ligand/Ch-Cl via a multi-component reaction strategy[68,69] (Figs. 3, 4). Also, a cooperative vinylogous anomeric-based oxidation pathway was suggested as plausible mechanism for the synthesis of new hybrid pyridines[70–84].

Results and discussion

A literature survey shows that in heterocyclic chemistry as a significant category of organic chemistry, pyridine plays as same as benzene in the concept of aromaticity. On the other hand, hybrid pyridines are the most hetero-cycle molecules which have been used for various purposes such as medicinal drugs, agricultural adducts, dyes, polymers etc.[85–88]. Therefore, development of hybrid pyridines is one of our main research interests. With this aim, herein we wish to report a new catalytic system for preparation of new hybrid pyridines with aryl, indole and sulfonate moieties.

After synthesis of Fe$_3$O$_4$@SiO$_2$@urea-riched ligand/Ch-Cl, we focused on the precise characterization of its structure. Firstly, FT-IR spectrum of catalyst were investigated (Fig. 5). According to FT-IR spectrum of Fe$_3$O$_4$@SiO$_2$@urea-riched ligand/Ch-Cl, the clear peak of C=O is appeared at 1665 cm^{-1}. The vibrational modes of Fe–O,
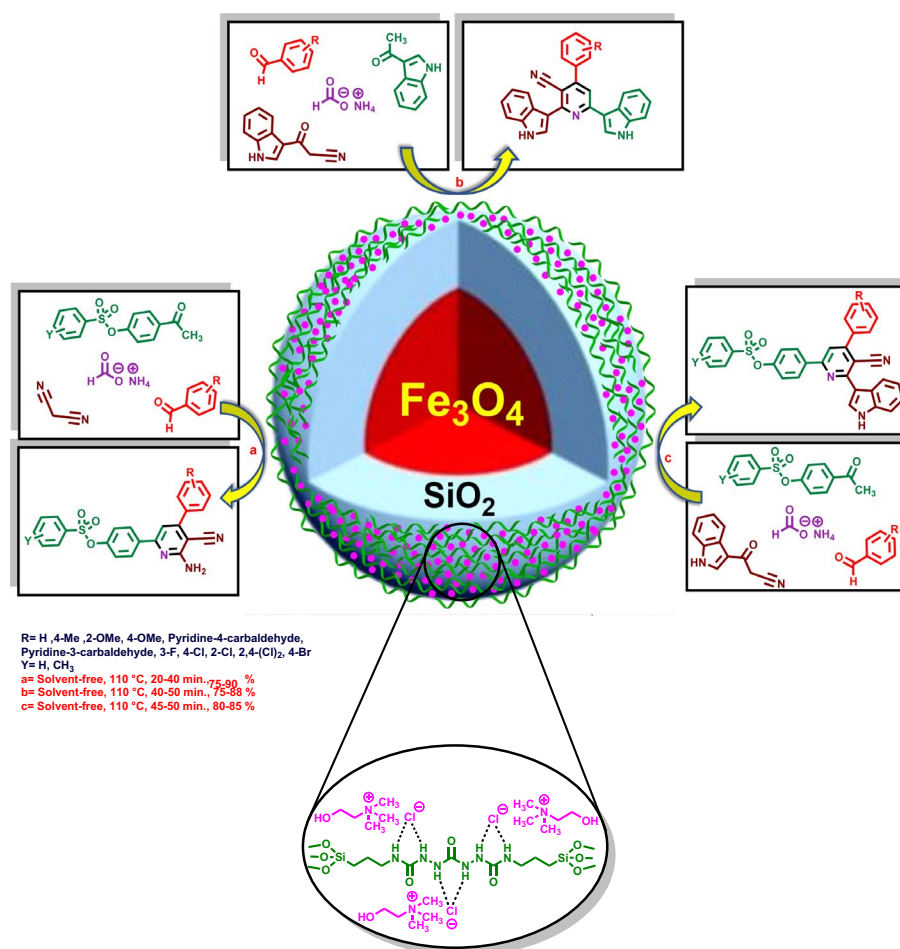

Figure 4. Synthesis of hybrid pyridines bearing indole and/or sulfonate moieties by using Fe$_3$O$_4$@SiO$_2$@urea-riched ligand/Ch-Cl as catalyst.

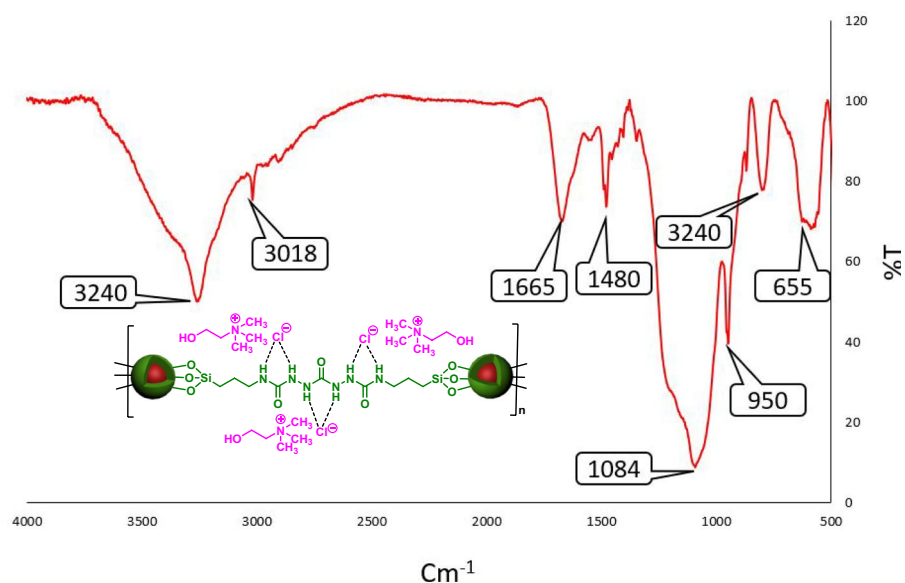**Figure 5.** FT-IR spectrum of Fe$_3$O$_4$@SiO$_2$@urea-riched ligand /Ch-Cl.

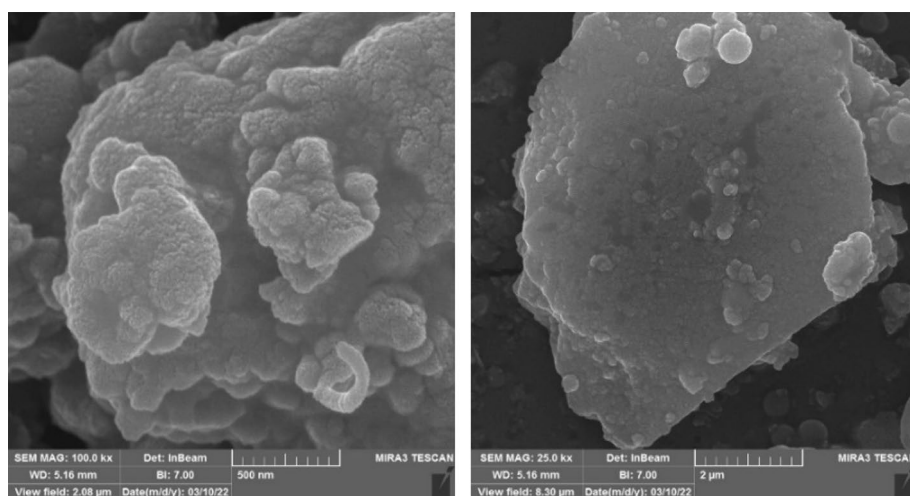**Figure 6.** FESEM images Fe$_3$O$_4$@SiO$_2$@urea-riched ligand/Ch-Cl.

Si–O and NH groups are respectively shown at 655, 1084 and 3240 cm^{-1}. Moreover, the broad peak about of 3200 cm^{-1} confirmed the existence of hydroxy group of Ch-Cl and free hydroxy groups in the surface of Fe$_3$O$_4$.

Field emission scanning electron microscopy (FESEM) analysis was recorded to check the morphology of Fe$_3$O$_4$@SiO$_2$@urea-riched ligand /Ch-Cl. According to relevant images (Fig. 6), catalyst has a spherical and uniform shapes and its size is in the range of nanometers. Also, TEM analysis was investigated to confirm the formation of the catalyst with spherical morphology and the presence of organic layers on the surface of magnetic nanoparticles is well confirmed (Fig. 7).

Energy-dispersive X-ray spectroscopy (EDS) analysis was used for the examination of expected elements within the catalyst structure. As predicted, the elements of C, N, O, Fe, Cl and Si are presented in the structure of desired catalyst (Fig. 8). In addition, elemental mapping analysis shows how the elements are dispersed and confirmed the existence of abovementioned expected elements in the structure of catalyst (Fig. 9).

For investigation of magnetic properties of target catalyst, VSM technique was performed for Fe$_3$O$_4$@SiO$_2$@urea-riched ligand/Ch-Cl. According to revealed results, the saturation magnetization of Fe$_3$O$_4$@SiO$_2$@urea-riched ligand/Ch-Cl is about 27 emu/g which is enough for the easy separation of the catalyst from the reaction mixture (Fig. 10).

Thermal stability is another important factor for MDES systems. Therefore, we investigated the thermal stability of the catalyst by using TGA/DTG analysis (Fig. 11). When the catalyst is exposed to the thermal conditions up to 600 °C, two main weight losses are observed at temperatures 255 and 443 °C. The poor weight losses below 110 °C is related to removing of trapped solvents and the significant weight losses at 255 °C is related to
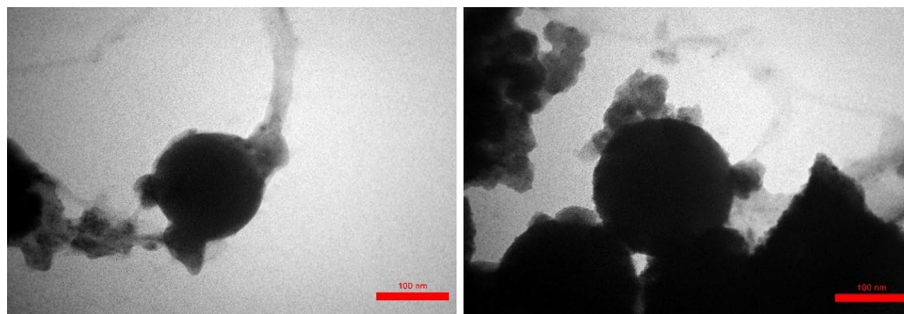
Figure 7. TEM images of Fe$_3$O$_4$@SiO$_2$@urea-riched ligand/Ch-Cl.

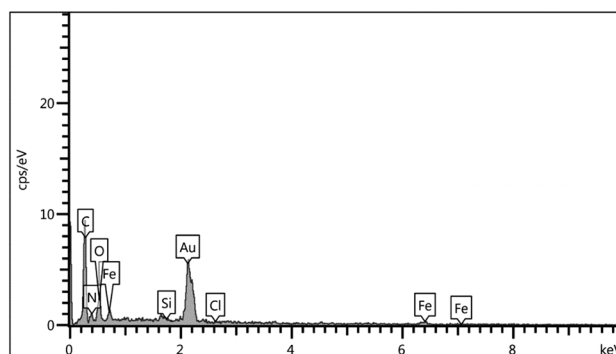**Figure 8.** EDS analysis diagram of Fe$_3$O$_4$@SiO$_2$@urea-riched ligand/Ch-Cl.

decomposition of organic layers. Therefore, it can be said that the catalyst is thermally stable up to this temperature. In an overview, the decrease in the weight of the catalyst by 30.59% indicates the presence of a significant amount of organic ligand on the Fe$_3$O$_4$ surface.

At the outset of the synthesis of hybrid pyridines, benzaldehyde, 4-acetylphenyl 4-methylbenzenesulfonate, malononitrile and ammonium format were chosen as model substrates for multi-component synthesis of pyridine derivatives. At the first, the reaction conducted in the presence of different amounts of catalyst such as 5, 10 and 20 mg. Also, the model reaction was tested in the absence of any catalyst. Anyway, the best result was obtained by using 10 mg of catalyst. Subsequent study on the effect of the temperature parameter displayed that 110 °C is the most suitable temperature to provide activation energy for the model reaction. After that, for the investigation of solvent effect, the model reaction was performed in several formal polar and nonpolar solvents and also, solvent free conditions. Nonetheless, due to high yield and low toxicity of reaction and simplicity of work up, solvent free conditions were chosen as proper conditions. More details are given in the Table 1. The bold values indicates the optimal reaction conditions.

In a separate study, the model reaction was performed in the presence of formal homogeneous DESs. For this purpose, several selected homogeneous DESs was prepared[89–94] and were used as catalyst for the model reaction. Distinguishingly, these materials have a good response to the synthesis of target molecule and all of products have a relatively good yield (Table 2). Nevertheless, devoid of suitable recycling and reusing of the catalyst in homogeneous systems is one of the defecting of these systems, while Fe$_3$O$_4$@SiO$_2$@urea-riched ligand/Ch-Cl as heterogeneous catalyst can easily recycled and reused.

For the validation of the importance of target catalyst, the model reaction was also performed in the presence of relative intermediates of Fe$_3$O$_4$@SiO$_2$@urea-riched ligand/Ch-Cl and some of formal catalysts such as Lewis acids, protic acids, hydrogen bond and basic catalysts. Using Fe$_3$O$_4$@SiO$_2$@urea-riched ligand/Ch-Cl as catalyst gave the best yield. It goes without saying that using of urea, thiourea and K$_2$CO$_3$ as catalyst have relatively good yield. Nevertheless, these catalysts do not have the ability to recycle and reuse, which are the basic capabilities of a complete catalyst. (Table 3).

In a comparative and precise study, for the investigation of the ability of ammonium format as reagent, we used several ammonium sources including ammonium format, ammonium acetate, ammonium sulfate, ammonium carbonate, ammonium florid, ammonium dichromate, ammonium chloride and ammonium nitrate upon model reaction. According to revealed results (Table 4), ammonium format revealed better performance for the synthesis of **1a** molecule.

Based on the in-hand results of optimization reactions, the generality of the reaction for synthesis of various hybrid pyridines was investigated. For this purpose, variety of aromatic aldehydes with electron-poor or electron-rich aryl groups, three different methyl ketones bearing indole or sulfonate groups and malononitrile or 3-(1*H*-indol-3-yl)-3-oxopropanenitrile were applied for the synthesis of hybrid pyridine derivatives. The
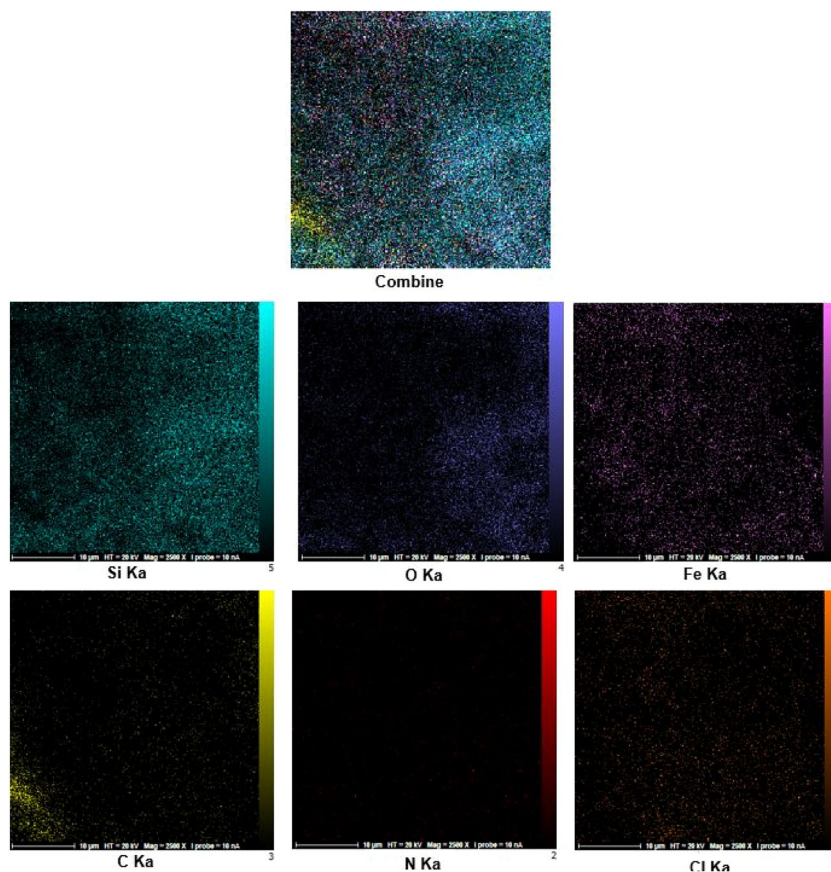
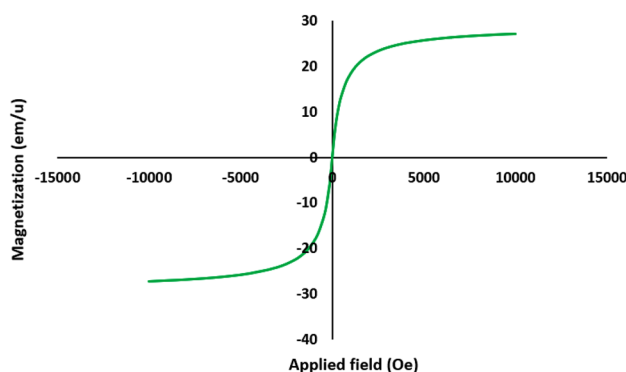**Figure 9.** Elemental mapping analysis of Fe_3O_4@SiO_2@urea-riched ligand/Ch-Cl.

Figure 10. Magnetization curves of Fe_3O_4@SiO_2@urea-riched ligand/Ch-Cl.

tolerance of the reaction to diverse starting materials displayed the broad application scope of the present route in the synthesis of complex hybrid pyridines (Table 5).

Based on our knowledge from the synthesis of hybrid pyridine rings, we suggested a plausible mechanism for the synthesis of **2c** (Fig. 12). At the first step, the carbonyl functional group of 4-acetylphenyl 4-methylbenzene-sulfonate is activated with catalyst and reacted with ammonia (arisen from thermal dissociation of ammonium format) and via a tautomerization process gives intermediate **A**. In another part of the reaction, aldehyde was activated by the catalyst and by a condensation reaction with 3-(1H-indol-3-yl)-3-oxopropanenitrile yields Knoevenagel intermediate (**B**). Subsequently, intermediate **A** was reacted with intermediate **B** and then via a tautomerization process, intermediate **C** was formed. Then, intermediate **C** undergoes intramolecular cyclization to gives intermediate **D**. In the next step, this intermediate undergoes a H_2O removing process which leads the formation of intermediate **E**. Finally, molecular H_2 (inert conditions) or H_2O_2 (air conditions) was released based on a cooperative vinylogous anomeric-based oxidation (CVABO)[70–84] to yields target molecule **2c**.
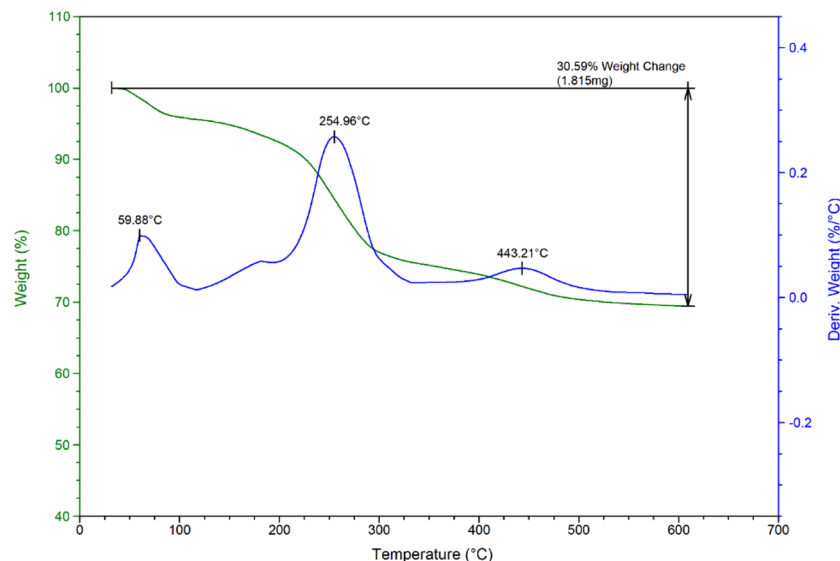
Figure 11. TGA/DTG curves of Fe_3O_4@SiO_2@urea-riched ligand/Ch-Cl.

Entry	Solvent	Temperature (°C)	Catalyst loading (mg)	Time (min.)	Yield (%)[b]
1[c]	–	**110**	**10**	**30**	**75**
2	–	110	20	40	60
3	–	110	5	70	50
4	–	110	–	60	20
5	–	110	–	120	38
6	–	100	10	50	80
7	–	90	10	70	70
8	–	80	10	100	40
9	–	70	10	180	35
10	H_2O	Reflux	10	60	–
11	EtOH	Reflux	10	60	50
12	n-Hexane	Reflux	10	60	–
13	EtOAc	Reflux	10	60	–
14	$CHCl_3$	Reflux	10	60	–

Table 1. Optimization of reaction conditions for synthesis of **1a**[a]. [a]Reaction conditions: 4-acetylphenyl 4-methylbenzenesulfonate (1 mmol, 0.290 g), malononitrile (1 mmol, 0.066 g), ammonium format (1.5 mmol, 0.094 g), benzaldehyde (1 mmol, 0.106 g), [b]Isolated yields. [c]Optimal data. Significant values are given in bold.

Magnetic substrates serve as ideal systems in recoverable catalysts and investigation of recycling and reusing potential of nanomagnetic catalyst is very important. Therefore, we examined the recycling and reusing ability of Fe_3O_4@SiO_2@urea-riched ligand/Ch-Cl for the synthesis of **1a** which leads to acceptable results. After running and performing each of reactions, the mixture of reaction was dissolved in CH_2Cl_2 and insoluble catalyst was separated from the reaction mixture and washed with CH_2Cl_2 (3×10 mL) and air dried. This work was conducted five times without significant reduction in yield of the reaction (Fig. 13). In addition, FT-IR spectrum was used for investigation the stability of recovered catalyst (See ESI).

Entry	Catalyst	The amount of catalyst	Yield (%)
1	Fe₃O₄@SiO₂@urea-riched ligand/Ch-Cl	10 mg	75
2	Ch-Cl/urea	10 mol%	77
3	Ch-Cl/thiourea	10 mol%	66
4	Ch-Cl/Citric acid	10 mol%	70
5	Ch-Cl/Benzamide	10 mol%	60
6	Ch-Cl/ Ascorbic acid	10 mol%	65
7	Ch-Cl/ Benzoic acid	10 mol%	70
8	Ch-Cl/Acetamide	10 mol%	60
9	Ch-Cl/ Glycerol	10 mol%	55

Table 2. Investigation of catalytic performance of selected homogeneous DESs upon model reaction for **1a**[a]. [a]Reaction conditions: 4-acetylphenyl 4-methylbenzenesulfonate (1 mmol, 0.290 g), malononitrile (1 mmol, 0.066 g), ammonium format (1.5 mmol, 0.094 g), benzaldehyde (1 mmol, 0.106 g), solvent-free, 110 °C, 30 min.

Entry	Catalyst	The amount of catalyst	Yield (%)
1	Fe₃O₄	10 mg	40
2	Fe₃O₄@SiO₂	10 mg	40
3	Fe₃O₄@SiO₂@urea-riched ligand	10 mg	70
4	Fe₃O₄@SiO₂@urea-riched ligand/Ch-Cl	10 mg	75
5	Ch-Cl	10 mol%	50
6	FeCl₃	10 mol%	50
7	Al(HSO₄)₃	10 mol%	45
8	Ca(HSO₄)₂	10 mol%	35
9	Zn(HSO₄)₂	10 mol%	35
10	Fe(HSO₄)₃	10 mol%	40
11	NH₂SO₃H	10 mol%	45
12	H₃BO₃	10 mol%	40
13	Urea	10 mol%	75
14	Thiourea	10 mol%	60
15	K₂CO₃	10 mol%	70
16	NaOH	10 mol%	Trace
17	C₅H₅N	10 mol%	45

Table 3. Comparative investigation of catalytic performance of Fe₃O₄@SiO₂@urea-riched ligand/Ch-Cl and its relative intermediates as well as some known catalysts upon model reaction for **1a**[a]. [a]Reaction conditions: 4-acetylphenyl 4-methylbenzenesulfonate (1 mmol, 0.290 g), malononitrile (1 mmol, 0.066 g), ammonium format (1.5 mmol, 0.094 g), benzaldehyde (1 mmol, 0.106 g), solvent-free, 110 °C, 30 min.

Entry	Reagent	Yield (%)
1	**NH₄HCO₂**	**75**
2	NH₄OAc	70
3	(NH₄)₂SO₄	–
4	(NH₄)₂CO₃	60
5	NH₄F	–
6	(NH₄)₂Cr₂O₇	50
7	NH₄Cl	–
8	NH₄NO₃	35

Table 4. Comparison of different ammonium sources as reagent upon model reaction for **1a**[a]. [a]Reaction conditions: 4-acetylphenyl 4-methylbenzenesulfonate (1 mmol, 0.290 g), malononitrile (1 mmol, 0.066 g), benzaldehyde (1 mmol, 0.106 g), ammonium source (1.5 mmol), solvent-free, 110 °C, 30 min. Significant values are given in bold.
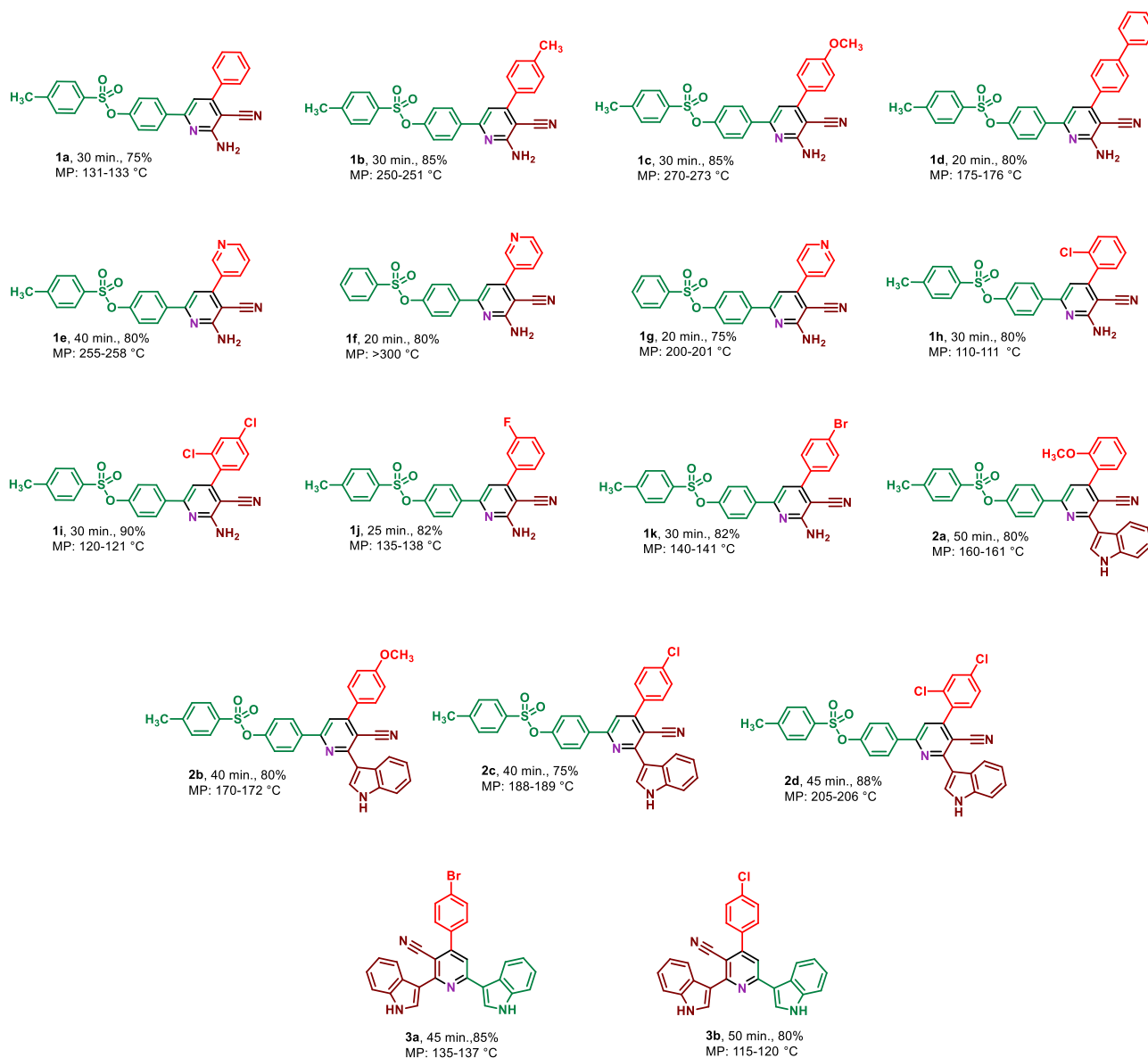
Table 5. Synthesis of hybrid pyridines with indole and sulfonate moieties by using Fe₃O₄@SiO₂@urea-riched ligand /Ch-Cl^a. ^{a}Reaction conditions: 4-acetylphenyl 4-methylbenzenesulfonate (1 mmol, 0.290 g) or 3-acetyl indole (1 mmol, 0.1590) malononitrile (1 mmol, 0.066 g) or 3-(1H-indol-3-yl)-3-oxopropanenitrile (1 mmol, 0.184 g), ammonium format (1.5 mmol, 0.094 g), benzaldehyde (1 mmol, 0.106 g), catalyst (10 mg), solvent-free, 110 °C.

Experimental section

Experimental procedure for the synthesis of Fe₃O₄@SiO₂@urea-riched ligand/Ch-Cl. At the first, Fe₃O₄@SiO₂@urea-riched ligand was synthesized according to our previous report[70–76]. Then, in a 100 mL round-bottomed flask 1 g of Fe₃O₄@SiO₂@urea-riched ligand and choline chloride (6 mmol, 0.837 g) and 100 mL of toluene as solvent were added and was refluxed for 24 h. After completing of reaction, the desired catalyst was separated by using external magnet and washed with n-hexane and EtOH several times and dried in air condition.

General experimental route for the synthesis of hybrid pyridine derivatives. In 10 mL round-bottomed flask methyl ketones (1 mmol), aromatic aldehydes (1 mmol), malononitrile (1 mmol, 0.066 g) or 3-(1H-indol-3-yl)-3-oxopropanenitrile (1 mmol, 0.184 g), ammonium format (1.5 mmol, 0.094 g) and 10 mg of catalyst were added and the mixture of reaction was stirred at 110 °C for appropriate times as indicated in Table 2. The progress of reactions was monitored by TLC techniques (n-hexane/ethylacetate, 6/4). After com-
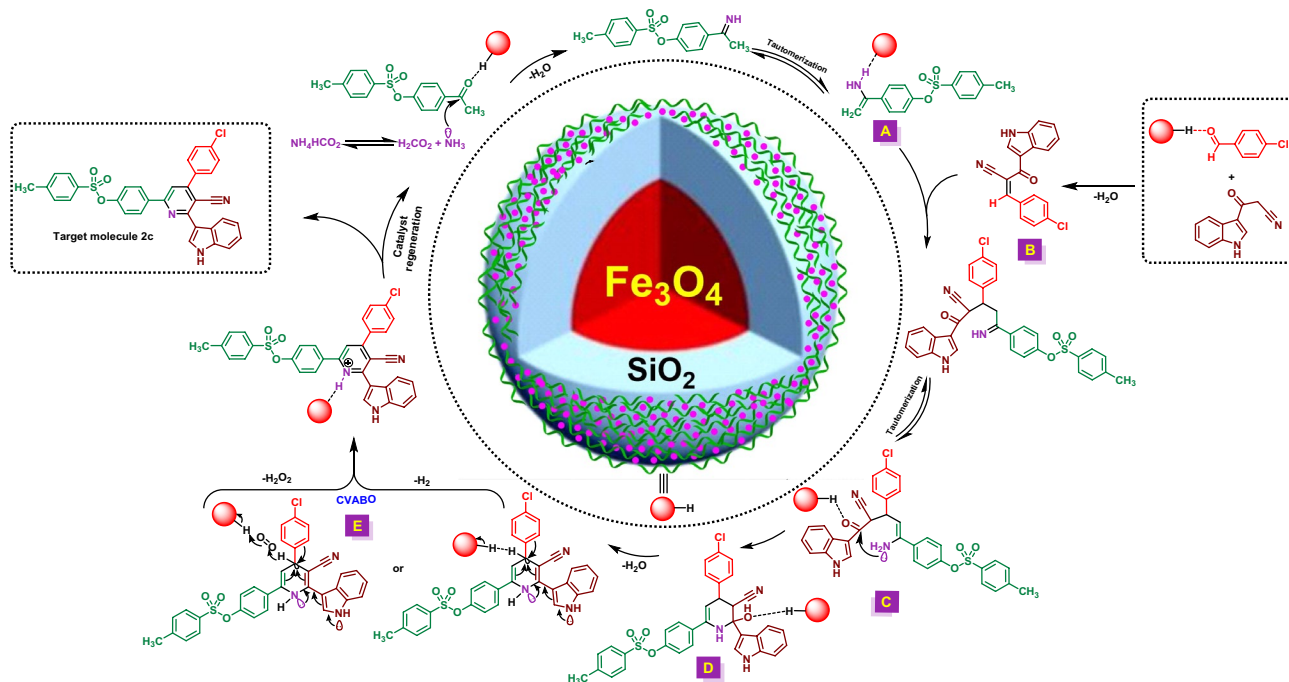
Figure 12. The plausible mechanism for the synthesis of **2c**.

pleting of each reaction, the mixture of reaction was dissolved in CH_2Cl_2 and the catalyst was separated from organic mixture. Then, each of products was purified by TLC plate techniques with *n*-hexane/ethyl acetate.

Spectral data. *4-(6-Amino-5-cyano-4-phenylpyridin-2-yl)phenyl 4-methylbenzenesulfonate (1a).* M.P. 131–133 °C, FT-IR (KBr, υ, cm^{-1}): 3489, 3367, 2209, 1597, 1493, 1091. ^{1}H NMR (250 MHz, DMSO$_{d6}$) δ$_{ppm}$ 8.10 (d, *J* = 10 Hz, 2H, Aromatic), 7.73 (d, *J* = 10 Hz, 2H, Aromatic), 7.65–7.62 (m, 2H, Aromatic), 7.52–7.43 (m, 5H, Aromatic), 7.23 (s, 1H, Aromatic), 7.15–7.03 (m, 4H, Aromatic and NH$_2$), 2.39 (s, 3H, CH$_3$). ^{13}C NMR (76 MHz, DMSO$_{d6}$) δ$_{ppm}$ 161.2, 157.5, 155.5, 150.7, 146.4, 137.0, 130.70, 130.10, 129.40, 129.2, 128.8, 122.7, 117.4, 109.8, 87.4, 21.6. MS (*m/z*) = calcd. for C$_{25}$H$_{19}$N$_3$O$_3$S: 441.5, found: 441.3.

4-(6-Amino-5-cyano-4-(p-tolyl)pyridin-2-yl)phenyl 4-methylbenzenesulfonate (1b). M.P. 250–251 °C, FT-IR (KBr, υ, cm^{-1}): 3508, 3391, 2922, 2206, 1367, 1153. ^{1}H NMR (301 MHz, DMSO$_{d6}$) δ$_{ppm}$ 8.14 (d, *J* = 9 Hz, 2H, Aromatic), 7.78 (d, *J* = 9 Hz, 2H, Aromatic), 7.59 (d, *J* = 9 Hz, 2H, Aromatic), 7.50 (d, *J* = 9 Hz, 2H, Aromatic), 7.37 (d, *J* = 6 Hz, 2H, Aromatic), 7.25 (s, 1H, Aromatic), 7.15 (d, *J* = 6 Hz, 2H, Aromatic), 7.04 (s, 2H, NH$_2$), 2.43 (s, 3H, CH$_3$), 2.41 (s, 3H, CH$_3$). ^{13}C NMR (76 MHz, DMSO$_{d6}$) δ$_{ppm}$ 161.3, 157.5, 155.5, 150.7, 146.4, 140.0, 137.1, 134.4, 131.7, 130.8, 129.8, 129.4, 128.8, 128.7, 122.7, 117.5, 109.7, 87.3, 21.7, 21.4. MS (*m/z*) = calcd. for C$_{26}$H$_{21}$N$_3$O$_3$S: 455.5, found: 455.2.

4-(6-Amino-5-cyano-4-(4-methoxyphenyl)pyridin-2-yl)phenyl 4-methylbenzenesulfonate (1c). M.P. 270–273 °C, FT-IR (KBr, υ, cm^{-1}): 3447, 3390, 2925, 2206, 1608, 1515, 1368, 1153. ^{1}H NMR (301 MHz, DMSO$_{d6}$) δ$_{ppm}$ 8.14 (d, *J* = 9 Hz, 2H, Aromatic), 7.79 (d, *J* = 9 Hz, 2H, Aromatic), 7.67 (d, *J* = 9 Hz, 2H, Aromatic), 7.50 (d, *J* = 9 Hz, 2H, Aromatic), 7.26 (s, 1H, Aromatic), 7.17 (s, 1H, Aromatic), 7.14 (s, 2H, Aromatic), 7.11 (s, 1H, Aromatic), 7.01 (s, 2H, NH$_2$), 3.86 (s, 3H, OCH$_3$), 2.44 (s, 3H, CH$_3$). ^{13}C NMR (76 MHz, DMSO$_{d6}$) δ$_{ppm}$ 161.4, 161.0, 157.4, 155.1, 150.6, 146.4, 140.9, 137.2, 131.7, 130.8, 130.4, 129.4, 128.8, 122.7, 117.7, 114.6, 109.6, 87.2, 55.9, 21.7. MS (*m/z*) = calcd. for C$_{26}$H$_{21}$N$_3$O$_4$S: 471.5, found: 471.2.

4-(4-([1,1'-Biphenyl]-4-yl)-6-amino-5-cyanopyridin-2-yl)phenyl 4-methylbenzenesulfonate (1d). M.P. 175–176 °C, FT-IR (KBr, υ, cm^{-1}): 3502, 3402, 2205, 1366, 1154. ^{1}H NMR (301 MHz, DMSO$_{d6}$) δ$_{ppm}$ 8.17 (d, *J* = 9 Hz, 2H, Aromatic), 7.88 (d, *J* = 9 Hz, 2H, Aromatic), 7.81–7.77 (m, 5H, Aromatic), 7.56–7.44 (m, 5H, Aromatic), 7.35 (s, 1H, Aromatic), 7.17 (d, *J* = 9 Hz, 2H), 7.10 (s, 2H, NH$_2$), 2.44 (s, 3H, CH$_3$). ^{13}C NMR (76 MHz, DMSO$_{d6}$) δ$_{ppm}$ 161.3, 157.6, 155.1, 150.7, 146.5, 141.9, 139.7, 137.1, 136.3, 131.7, 130.8, 129.6, 129.5, 128.8, 128.5, 127.4, 127.3, 122.7, 117.5, 109.8, 87.3, 21.7. MS (*m/z*) = calcd. for C$_{31}$H$_{23}$N$_3$O$_3$S: 517.6, found: 517.3.

4-(6'-Amino-5'-cyano-[3,4'-bipyridin]-2'-yl)phenyl 4-methylbenzenesulfonate (1e). M.P. 255–258 °C, FT-IR (KBr, υ, cm^{-1}): 3442, 3373, 2925, 2213, 1369, 1153. ^{1}H NMR (301 MHz, DMSO$_{d6}$) δ$_{ppm}$ 8.88 (dd, *J* = 3, 0.8 Hz, 1H), 8.75 (dd, *J* = 6, 3 Hz, 1H), 8.17 (m, 2H), 8.12 (m, 1H, Aromatic), 7.97 (s, 1H, Aromatic), 7.79 (d, *J* = 9 Hz, 2H, Aromatic), 7.61 (ddd, *J* = 7.9, 4.8, 0.9 Hz, 1H, Aromatic), 7.50 (d, *J* = 6 Hz, 2H), 7.38 (s, 1H, Aromatic), 7.18 (s, 2H, NH$_2$), 7.15 (s, 1H, Aromatic), 2.44 (s, 3H, CH$_3$). MS (*m/z*) = calcd. for C$_{24}$H$_{18}$N$_4$O$_3$S: 442.5, found: 442.2.

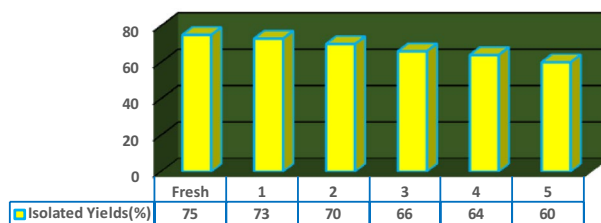**Figure 13.** Diagram of recycling and reusing of $Fe_3O_4@SiO_2@$urea-riched ligand/Ch-Cl in the synthesis of **1a**.

4-(6'-Amino-5'-cyano-[3,4'-bipyridin]-2'-yl)phenyl benzenesulfonate (1f). M.P. > 300 °C, FT-IR (KBr, υ, cm^{-1}): 3426, 3317, 3168, 2212, 1642, 1448, 1354, 1152. ^{1}H NMR (250 MHz, DMSO$_{d6}$) δ_{ppm} 8.84–8.80 (m, 1H, Aromatic), 8.70 (d, J = 5 Hz, 1H, Aromatic), 8.13 (d, J = 7.5 Hz, 2H, Aromatic), 7.92–7.79 (m, 3H, Aromatic), 7.69–7.66 (m, 3H, Aromatic), 7.60–7.54 (m, 1H, Aromatic), 7.34 (s, 1H, Aromatic), 7.20–7.11 (m, 4H, Aromatic and NH$_2$). ^{13}C NMR (76 MHz, DMSO$_{d6}$) δ_{ppm} 161.0, 157.8, 151.0, 149.1, 136.6, 136.5, 135.6, 132.1, 130.8, 130.3, 129.5, 128.7, 124.0, 122.7, 119.1, 117.1, 116.1, 109.9, 87.4. MS (m/z) = calcd. for C$_{23}$H$_{16}$N$_4$O$_3$S: 428.5, found: 428.3.

4-(6-Amino-5-cyano-[4,4'-bipyridin]-2-yl)phenylbenzenesulfonate (1g). M.P. 200–201 °C, FT-IR (KBr, υ, cm^{-1}): 3442, 3291, 3170, 2216, 1375, 1153. ^{1}H NMR (301 MHz, DMSO) δ_{ppm} 8.75 (d, J = 6 Hz, 2H, Aromatic), 7.94 (dd, J = 6, 1.3 Hz, 2H, Aromatic), 7.74–7.65 (m, 8H, Aromatic), 7.23 (d, J = 9 Hz, 2H, Aromatic), 7.03 (s, 2H, NH$_2$). ^{13}C NMR (76 MHz, DMSO$_{d6}$) δ_{ppm} 154.5, 150.5, 150.2, 149.2, 147.6, 145.2, 136.8, 135.7, 134.8, 131.1, 130.5, 128.7, 123.7, 122.8, 118.7, 95.6. MS (m/z) = calcd. for C$_{23}$H$_{16}$N$_4$O$_3$S: 428.5, found: 428.4.

4-(6-Amino-4-(2-chlorophenyl)-5-cyanopyridin-2-yl)phenyl 4-methylbenzenesulfonate (1h). M.P. 110–111 °C, FT-IR (KBr, υ, cm^{-1}): 3489, 3373, 3168, 2918, 2213, 1370, 1153. ^{1}H NMR (301 MHz, DMSO$_{d6}$) δ_{ppm} 8.13 (d, J = 9 Hz, 2H, Aromatic), 7.77 (d, J = 6 Hz, 2H, Aromatic), 7.68–7.65 (m, 1H, Aromatic), 7.53–7.48 (m, 5H, Aromatic), 7.23 (s, 1H, Aromatic), 7.20–7.13 (m, 4H, Aromatic and NH$_2$), 2.43 (s, 3H, CH$_3$). ^{13}C NMR (76 MHz, DMSO$_{d6}$) δ_{ppm} 160.1, 157.5, 153.8, 150.8, 146.5, 136.8, 136.5, 131.7, 131.4, 131.1, 130.8, 130.2, 129.4, 129.1, 128.8, 128.0, 122.8, 116.4, 110.3, 89.3, 21.7. MS (m/z) = calcd. for C$_{25}$H$_{18}$ClN$_3$O$_3$S: 475.9, found: 475.2.

4-(6-Amino-5-cyano-4-(2,4-dichlorophenyl)pyridin-2-yl)phenyl 4-methylbenzenesulfonate (1i). M.P. 120–121 °C, FT-IR (KBr, υ, cm^{-1}): 3485, 3376, 2925, 2213, 1502, 1447, 1371, 1153. ^{1}H NMR (301 MHz, DMSO$_{d6}$) δ_{ppm} 8.12 (d, J = 9 Hz, 2H, Aromatic), 7.88 (d, J = 1.9 Hz, 1H, Aromatic), 7.77 (d, J = 6 Hz, 2H, Aromatic), 7.63 (dd, J = 9, 3 Hz, 1H, Aromatic), 7.57 (s, 1H, Aromatic), 7.50 (d, J = 9 Hz, 2H, Aromatic), 7.25 (s, 1H, Aromatic), 7.21 (s, 2H, NH$_2$), 7.15 (d, J = 9 Hz, 2H, Aromatic), 2.43 (s, 3H, CH$_3$). ^{13}C NMR (76 MHz, DMSO$_{d6}$) δ_{ppm} 160.5, 157.7, 152.7, 150.8, 146.5, 136.7, 135.5, 135.3, 133.0, 132.5, 131.7, 130.8, 129.7, 129.4, 128.8, 128.3, 122.8, 116.3, 110.2, 89.1, 21.7. MS (m/z) = calcd. for C$_{25}$H$_{17}$Cl$_2$N$_3$O$_3$S: 510.4, found: 510.3.

4-(6-Amino-5-cyano-4-(3-fluorophenyl)pyridin-2-yl)phenyl 4-methylbenzenesulfonate (1j). M.P. 135–138 °C, FT-IR (KBr, υ, cm^{-1}): 3475, 3382, 2211, 1615, 1447, 1369, 1153. ^{1}H NMR (301 MHz, DMSO$_{d6}$) δ_{ppm} 8.16 (d, J = 9 Hz, 2H, Aromatic), 7.79 (d, J = 9 Hz, 2H, Aromatic), 7.59 (s, 1H, Aromatic), 7.55 (s, 1H, Aromatic), 7.51–7.49 (m, 3H, Aromatic), 7.43–7.37 (m, 1H, Aromatic), 7.32 (s, 1H, Aromatic), 7.17 (s, 1H, Aromatic), 7.14–7.13 (m, 3H, Aromatic and NH$_2$), 2.44 (s, 3H, CH$_3$). ^{13}C NMR (76 MHz, DMSO$_{d6}$) δ_{ppm} 164.1, 161.2, 157.8, 154.1, 150.8, 146.5, 139.5, 139.4, 136.9, 131.7, 130.8, 129.5, 128.8, 125.1, 122.7, 117.2, 116.8, 116.1, 115.7, 109.9, 87.4, 21.7. MS (m/z) = calcd. for C$_{25}$H$_{18}$FN$_3$O$_3$S: 459.5, found: 459.2.

4-(6-Amino-4-(4-bromophenyl)-5-cyanopyridin-2-yl)phenyl 4-methylbenzenesulfonate (1k). M.P. 140–141 °C, FT-IR (KBr, υ, cm^{-1}): 3479, 3380, 2923, 2213, 1594, 1492, 1370, 1153. ^{1}H NMR (301 MHz, DMSO$_{d6}$) δ_{ppm} 8.14 (d, J = 9 Hz, 2H, Aromatic), 7.78 (d, J = 6 Hz, 4H, Aromatic), 7.65 (d, J = 9 Hz, 2H, Aromatic), 7.50 (d, J = 9 Hz, 2H, Aromatic), 7.29 (s, 1H, Aromatic), 7.17–7.12 (m, 4H, Aromatic, NH$_2$), 2.44 (s, 3H, CH$_3$). ^{13}C NMR (76 MHz, DMSO$_{d6}$) δ_{ppm} 161.2, 157.7, 154.4, 150.7, 146.5, 137.0, 136.4, 132.2, 131.7, 131.0, 130.8, 129.5, 128.8, 123.8, 122.7, 117.2, 116.2, 109.7, 87.2, 21.7. MS (m/z) = calcd. for C$_{25}$H$_{18}$BrN$_3$O$_3$S: 520.4, found: 521.1.

4-(5-Cyano-6-(1H-indol-3-yl)-4-(2-methoxyphenyl)pyridin-2-yl)phenyl 4-methylbenzenesulfonate (2a). M.P. 160–161 °C, FT-IR (KBr, υ, cm^{-1}): 3396, 2928, 2223, 1374, 1168. ^{1}H NMR (301 MHz, DMSO$_{d6}$) δ_{ppm} 11.92 (s, 1H, NH), 8.34 (d, J = 9 Hz, 4H, Aromatic), 7.90 (s, 1H, Aromatic), 7.82 (d, J = 9 Hz, 2H, Aromatic), 7.59–7.56 (m, 2H, Aromatic), 7.54–7.48 (m, 3H, Aromatic), 7.28–7.23 (m, 5H, Aromatic), 7.17 (t, J = 9 Hz, 1H, Aromatic), 3.85 (s, 3H, OCH$_3$), 2.44 (s, 3H, CH$_3$). ^{13}C NMR (76 MHz, DMSO$_{d6}$) δ_{ppm} 158.6, 157.2, 157.0, 156.6, 153.6, 150.9, 146.5, 137.1, 136.9, 131.8, 130.9, 129.6, 128.9, 128.7, 126.4, 126.2, 123.1, 122.9, 121.7, 121.3, 121.2, 118.9, 118.0, 113.3, 112.6, 112.3, 104.3, 56.1, 21.7. MS (m/z) = calcd. for C$_{34}$H$_{25}$N$_3$O$_4$S: 571.6, found: 571.3.

4-(5-Cyano-6-(1H-indol-3-yl)-4-(4-methoxyphenyl)pyridin-2-yl)phenyl 4-methylbenzenesulfonate (2b). M.P. 170–172 °C, FT-IR (KBr, υ, cm^{-1}): 3402, 2900, 2211, 1368, 1153. ^{1}H NMR (301 MHz, DMSO$_{d6}$) δ_{ppm} 11.89 (s,

1H, NH), 8.38–8.32 (m, 4H, Aromatic), 7.94 (s, 1H, Aromatic), 7.84–7.80 (m, 4H, Aromatic), 7.58–7.50 (m, 4H, Aromatic), 7.27 (d, $J = 9$ Hz, 3H, Aromatic), 7.19 (d, $J = 9$ Hz, 2H, Aromatic), 3.89 (s, 3H, OCH$_3$), 2.45 (s, 3H, CH$_3$). ^{13}C NMR (76 MHz, DMSO$_{d6}$) δ_{ppm} 161.1, 158.0, 157.2, 155.3, 150.9, 146.5, 137.2, 136.8, 131.8, 131.0, 130.8, 129.7, 129.3, 128.8, 126.5, 123.1, 122.9, 121.7, 121.3, 119.6, 116.9, 114.7, 113.4, 112.6, 102.1, 55.9, 21.7. MS (m/z) = calcd. for C$_{34}$H$_{25}$N$_3$O$_4$S: 571.6, found: 571.3.

4-(4-(4-Chlorophenyl)-5-cyano-6-(1H-indol-3-yl)pyridin-2-yl)phenyl 4-methylbenzenesulfonate (2c). M.P. 188–189 °C, FT-IR (KBr, υ, cm^{-1}): 3362, 2922, 2213, 1596, 1433, 1365, 1150. ^{1}H NMR (301 MHz, DMSO$_{d6}$) δ_{ppm} 11.90 (s, 1H, NH), 8.39–8.32 (m, 4H, Aromatic), 7.98 (s, 1H, Aromatic), 7.88–7.81 (m, 4H, Aromatic), 7.71 (d, $J = 9$ Hz, 2H, Aromatic), 7.58 (d, $J = 9$ Hz, 1H, Aromatic), 7.51 (d, $J = 9$ Hz, 2H, Aromatic), 7.28–7.24 (m, 4H, Aromatic), 2.44 (s, 3H, CH$_3$). MS (m/z) = calcd. for C$_{33}$H$_{22}$ClN$_3$O$_3$S: 576.1, found: 576.2.

4-(5-Cyano-4-(2,4-dichlorophenyl)-6-(1H-indol-3-yl)pyridin-2-yl)phenyl 4-methylbenzenesulfonate (2d). M.P. 205–206 °C, FT-IR (KBr, υ, cm^{-1}): 3424, 2221, 1619, 1432, 750. ^{1}H NMR (301 MHz, DMSO$_{d6}$) δ_{ppm} 12.00 (s, 1H, NH), 8.39– 8.34 (m, 4H, Aromatic), 8.00 (s, 1H, Aromatic), 7.95 (s, 1H, Aromatic), 7.82 (d, $J = 9$ Hz, 2H, Aromatic), 7.71 (s, 2H, Aromatic), 7.58 (d, $J = 6$ Hz, 1H, Aromatic), 7.51 (d, $J = 9$ Hz, 2H, Aromatic), 7.29–7.26 (m, 4H, Aromatic), 2.44 (s, 3H, CH$_3$). ^{13}C NMR (76 MHz, DMSO$_{d6}$) δ_{ppm} 162.3, 157.5, 152.7, 151.1, 146.5, 136.9, 135.6, 135.2, 133.2, 132.9, 131.8, 130.8, 129.7, 129.2, 128.8, 128.4, 126.3, 123.2, 121.8, 121.5, 118.2, 117.5, 113.1, 112.7, 103.4, 21.7.

4-(4-Bromophenyl)-2,6-di(1H-indol-3-yl) nicotinonitrile (3a). M.P. 135–137 °C, ^{1}H NMR (301 MHz, DMSO$_{d6}$) δ_{ppm} 11.94 (s, 1H, NH), 11.82 (s, 1H, NH), 8.63 (d, $J = 9$ Hz, 1H, Aromatic), 8.53 (d, $J = 3$ Hz, 1H, Aromatic), 8.37 (d, $J = 9$ Hz, 1H, Aromatic), 8.30 (d, $J = 3$ Hz, 1H, Aromatic), 7.90 (s, 1H, Aromatic), 7.85 (d, $J = 9$ Hz, 2H, Aromatic), 7.78 (d, $J = 9$ Hz, 2H, Aromatic), 7.61 (d, $J = 9$ Hz, 1H, Aromatic), 7.54 (d, $J = 9$ Hz, 1H, Aromatic), 7.32–7.20 (m, 3H, Aromatic), 7.10 (t, $J = 9$ Hz, 1H, Aromatic). ^{13}C NMR (76 MHz, DMSO$_{d6}$) δ_{ppm} 158.4, 158.1, 152.6, 137.8, 136.9, 132.1, 131.5, 129.9, 128.7, 126.5, 125.8, 123.6, 122.8, 122.6, 121.9, 121.1, 120.8, 119.7, 115.8, 115.3, 114.1, 112.5, 98.8. MS (m/z) = calcd. for C$_{28}$H$_{17}$BrN$_4$: 489.4, found: 489.1.

4-(4-Chlorophenyl)-2,6-di(1H-indol-3-yl) nicotinonitrile (3b). M.P. 115–120 °C, FT-IR (KBr, υ, cm^{-1}): 3391, 2959, 2217, 731. ^{1}H NMR (301 MHz, DMSO$_{d6}$) δ_{ppm} 11.92 (s, 1H, NH), 11.81 (s, 1H, NH), 8.61 (d, $J = 9$ Hz, 1H, Aromatic), 8.53 (d, $J = 9$ Hz, 1H, Aromatic), 8.34 (d, $J = 9$ Hz, 1H, Aromatic), 8.28 (d, $J = 6$ Hz, 1H, Aromatic), 7.90 (s, 1H, Aromatic), 7.86 (d, $J = 9$ Hz, 2H, Aromatic), 7.71 (d, $J = 6$ Hz, 2H, Aromatic), 7.59 (d, $J = 6$ Hz, 1H, Aromatic), 7.52 (d, $J = 9$ Hz, 1H, Aromatic), 7.30–7.16 (m, 3H, Aromatic), 7.09 (t, $J = 9$ Hz, 1H, Aromatic). MS (m/z) = calcd. for C$_{28}$H$_{17}$ClN$_4$: 444.9, found: 444.2.

Conclusion

In summary, we reported the design, synthesis and characterization of a new heterogeneous catalytic system namely [Fe$_3$O$_4$@SiO$_2$@urea-riched ligand/Ch-Cl]. The revealed results from characterization of this compound such as FT-IR, FESEM, TEM, EDS-Mapping, TGA/DTG and VSM analysis show its successful synthesis. This system has an excellent catalytical potential for synthesis of hybrid pyridines containing sulfonate or indole sections. In this method several starting materials were used for the synthesis of hybrid pyridine rings which yield divers products in mild reaction conditions. Besides, cooperative vinylogous anomeric-based oxidation pathway was suggested as a rational mechanism for the synthesis of hybrid pyridine (Supplementary Information S1).

Data availability

All data generated or analyzed during this study are included in this published article [and its supplementary information files].

References

1. Hansen, B. B. *et al.* Deep eutectic solvents: A review of fundamentals and applications. *Chem. Rev.* **121**, 1232–1285 (2020).
2. Smith, E. L., Abbott, A. P. & Ryder, K. S. Deep eutectic solvents (DESs) and their applications. *Chem. Rev.* **114**, 11060–11082 (2014).
3. Vilková, M., Płotka-Wasylka, J. & Andruch, V. The role of water in deep eutectic solvent-base extraction. *J. Mol. Liq.* **304**, 112747 (2020).
4. Atilhan, M. & Aparicio, S. Review and perspectives for effective solutions to grand challenges of energy and fuels technologies via novel deep eutectic solvents. *Energy Fuels* **35**, 6402–6419 (2021).
5. Van Osch, D. J., Dietz, C. H., Warrag, S. E. & Kroon, M. C. The curious case of hydrophobic deep eutectic solvents: A story on the discovery, design, and applications. *ACS Sustain. Chem. Eng.* **8**, 10591–10612 (2020).
6. Ge, X., Gu, C., Wang, X. & Tu, J. Deep eutectic solvents (DESs)-derived advanced functional materials for energy and environmental applications: Challenges, opportunities, and future vision. *J. Mater. Chem. A* **5**, 8209–8229 (2017).
7. Hooshmand, S. E., Afshari, R., Ramón, D. J. & Varma, R. S. Deep eutectic solvents: Cutting-edge applications in cross-coupling reactions. *Green Chem.* **22**, 3668–3692 (2020).
8. García-Álvarez, J. Deep eutectic mixtures: Promising sustainable solvents for metal-catalysed and metal-mediated organic reactions. *Eur. J. Inorg. Chem.* **2015**, 5147–5157 (2015).
9. Zamani, P. *et al.* Magnetic nanoparticle anchored deep eutectic solvents as a catalyst for the etherification and amination of naphthols. *Adv. Synth. Catal.* **360**, 4372–4380 (2018).
10. Wu, S., Cai, C., Li, F., Tan, Z. & Dong, S. Deep eutectic supramolecular polymers: Bulk supramolecular materials. *Angew. Chem. Int. Ed.* **59**, 11871–11875 (2020).

11. Akbarian, M., Sanchooli, E., Oveisi, A. R. & Daliran, S. Choline chloride-coated UiO-66-Urea MOF: A novel multifunctional heterogeneous catalyst for efficient one-pot three-component synthesis of 2-amino-4*H*-chromenes. *J. Mol. Liq.* **325**, 115228–115239 (2021).

12. Aguirre, M. Á. & Canals, A. Magnetic deep eutectic solvents in microextraction techniques. *Trends Analyt. Chem.* **146**, 116500 (2022).

13. Le Nguyen, T. T. An efficient multicomponent synthesis of 2, 4, 5-trisubstituted and 1, 2, 4, 5-tetrasubstituted imidazoles catalyzed by a magnetic nanoparticle supported Lewis acidic deep eutectic solvent. *RSC Adv.* **9**, 38148–38153 (2019).

14. Maia, R. A., Louis, B. & Baudron, S. A. Deep eutectic solvents for the preparation and post-synthetic modification of metal-and covalent organic frameworks. *CrystEngComm* **23**, 5016–5032 (2021).

15. Santana-Mayor, Á., Rodríguez-Ramos, R., Socas-Rodríguez, B., Afonso, M. D. M. & Palenzuela, J. A. Combinations of nanomaterials and deep eutectic solvents as innovative materials in food analysis. *Processes* **9**, 2131 (2021).

16. Xu, K. *et al.* Magnetic solid-phase extraction of protein with deep eutectic solvent immobilized magnetic graphene oxide nanoparticles. *Talanta* **148**, 153–162 (2016).

17. Kalaj, M. & Cohen, S. M. Postsynthetic modification: An enabling technology for the advancement of metal-organic frameworks. *ACS cent. Sci.* **6**, 1046–1057 (2020).

18. Sadiq, A. C., Olasupo, A., Rahim, N. Y., Ngah, W. S. W. & Suah, F. B. M. Comparative removal of malachite green dye from aqueous solution using deep eutectic solvents modified magnetic chitosan nanoparticles and modified protonated chitosan beads. *J. Environ. Chem. Eng.* **9**, 106281 (2021).

19. Bide, Y. & Shokrollahzadeh, S. Toward tailoring of a new draw solute for forward osmosis process: Branched poly (deep eutectic solvent)-decorated magnetic nanoparticles. *J. Mol. Liq.* **320**, 114409 (2020).

20. Li, L. *et al.* Deep eutectic solvents functionalized polymers for easily and efficiently promoting biocatalysis. *J. Catal.* **374**, 306–319 (2019).

21. Li, Z. *et al.* Deep eutectic solvents appended to UiO-66 type metal organic frameworks: Preserved open metal sites and extra adsorption sites for CO_2 capture. *Appl. Surf. Sci.* **480**, 770–778 (2019).

22. Cruz, H., Pinto, A. L., Jordão, N., Neves, L. A. & Branco, L. C. Alkali iodide deep eutectic solvents as alternative electrolytes for dye sensitized solar cells. *Sustain. Chem.* **2**, 222–236 (2021).

23. Pateli, I. M., Abbott, A. P., Jenkin, G. R. & Hartley, J. M. Electrochemical oxidation as alternative for dissolution of metal oxides in deep eutectic solvents. *Green Chem.* **22**, 8360–8368 (2020).

24. Ma, Q. *et al. Electrochim. Acta* **353**, 136486–136495 (2020).

25. Mahanta, U. *et al.* Ionic-liquid-based deep eutectic solvents as novel electrolytes for supercapacitors: COSMO-SAC predictions, synthesis, and characterization. *ACS Sustain. Chem. Eng.* **8**, 372–381 (2019).

26. Svigelj, R., Dossi, N., Grazioli, C. & Toniolo, R. Deep eutectic solvents (DESs) and their application in biosensor development. *Sensors* **21**, 4263–4281 (2021).

27. Yang, X. *et al.* Deep eutectic solvents as efficient catalysts for fixation of CO_2 to cyclic carbonates at ambient temperature and pressure through synergetic catalysis. *ACS Sustain. Chem. Eng.* **9**, 10437–10443 (2021).

28. Shaabani, A. & Afshari, R. Magnetic Ugi-functionalized graphene oxide complexed with copper nanoparticles: efficient catalyst toward Ullman coupling reaction in deep eutectic solvents. *J. Colloid Interface Sci.* **510**, 384–394 (2018).

29. Kiani, A. Alinezhad, H. & Ghasemi, S. Embedded palladium nanoparticles on metal–organic framework/covalently sulfonated magnetic SBA-15 mesoporous silica composite: As a highly proficient nanocatalyst for Suzuki–Miyaura coupling reaction in amino acid-based natural deep eutectic solvent. *Appl. Organomet. Chem.* e6912 (2022).

30. Makoś-Chełstowska, P., Kaykhaii, M., Płotka-Wasylka, J. & de la Guardia, M. Magnetic deep eutectic solvents—Fundamentals and applications. *J. Mol. Liq.* **365**, 120158–120170 (2022).

31. Bakhtiarian, M. & Khodaei, M. M. Synthesis of 2, 3-dihydro-4 (1*H*) quinazolinones using a magnetic pectin-supported deep eutectic solvent. *Colloids Surf. A Physicochem. Eng. Asp.* **641**, 128569 (2022).

32. Shaibuna, M., Theresa, L. V. & Sreekumar, K. Neoteric deep eutectic solvents: History, recent developments, and catalytic applications. *Soft Matter* **18**, 2695–2721 (2022).

33. Longo, L. S. Jr. & Craveiro, M. V. Deep eutectic solvents as unconventional media for multicomponent reactions. *J. Braz. Chem. Soc.* **29**, 1999–2025 (2018).

34. Tran, P. H. One-pot multicomponent synthesis of thieno [2, 3-*b*] indoles catalyzed by a magnetic nanoparticle-supported [Urea] 4 [$ZnCl_2$] deep eutectic solvent. *RSC Adv.* **10**, 9663–9671 (2020).

35. Liu, P., Hao, J. W., Mo, L. P. & Zhang, Z. H. Recent advances in the application of deep eutectic solvents as sustainable media as well as catalysts in organic reactions. *RSC Adv.* **5**, 48675–48704 (2015).

36. Anizadeh, M. R., Zolfigol, M. A., Torabi, M., Yarie, M. & Notash, B. *J. Mol. Liq.* **364**, 120016–120027 (2022).

37. Abtahi, B. & Tavakol, H. Choline chloride-urea deep eutectic solvent as an efficient media for the synthesis of propargylamines via organocuprate intermediate. *Appl. Organometal. Chem.* **34**, e5895 (2020).

38. Lin, Y. F. & Sun, I. W. Electrodeposition of zinc from a Lewis acidic zinc chloride-1-ethyl-3-methylimidazolium chloride molten salt. *Electrochim. Acta* **44**, 2771–2777 (1999).

39. Zamani, P. & Khosropour, A. R. A combination of natural deep eutectic solvents and microflow technology: A sustainable innovation for the tandem synthesis of 3-aminohexahydrocoumarins. *Green Chem.* **18**, 6450–6455 (2016).

40. Cui, Y., Li, C. & Bao, M. Deep eutectic solvents (DESs) as powerful and recyclable catalysts and solvents for the synthesis of 3, 4-dihydropyrimidin-2 (1H)-ones/thiones. *Green Process. Synth.* **8**, 568–576 (2019).

41. Ma, Z., Mohapatra, J., Wei, K., Liu, J. P. & Sun, S. Magnetic nanoparticles: Synthesis, anisotropy, and applications. *Chem. Rev.* **123**, 3904–3943 (2021).

42. Garcia-Merino, B., Bringas, E. & Ortiz, I. Synthesis and applications of surface-modified magnetic nanoparticles: Progress and future prospects. *Rev. Chem. Eng.* **38**, 821–842 (2022).

43. Liu, S., Yu, B., Wang, S., Shen, Y. & Cong, H. Preparation, surface functionalization and application of Fe_3O_4 magnetic nanoparticles. *Adv. Colloid Interface Sci.* **281**, 102165 (2020).

44. Mohamed Noor, M. H., Wong, S., Ngadi, N., Mohammed Inuwa, I. & Opotu, L. A. Assessing the effectiveness of magnetic nanoparticles coagulation/flocculation in water treatment: A systematic literature review. *Int. J. Sci. Environ. Technol.* **19**, 6935–6956 (2022).

45. Mittal, A., Roy, I. & Gandhi, S. Magnetic nanoparticles: An overview for biomedical applications. *Magnetochemistry* **8**, 107 (2022).

46. Zhou, K., Zhou, X., Liu, J. & Huang, Z. Application of magnetic nanoparticles in petroleum industry: A review. *J. Pet. Sci. Eng.* **188**, 106943 (2020).

47. Verma, S., Kujur, S., Sharma, R. & Pathak, D. D. Cucurbit [6] uril-supported Fe_3O_4 magnetic nanoparticles catalyzed green and sustainable synthesis of 2-substituted benzimidazoles via acceptorless dehydrogenative coupling. *ACS Omega* **7**, 9754–9764 (2022).

48. Wu, L., Mendoza-Garcia, A., Li, Q. & Sun, S. Organic phase syntheses of magnetic nanoparticles and their applications. *Chem. Rev.* **116**, 10473–10512 (2016).

49. Xiong, G. Chen, X. L., You, L. X., Ren, B. Y., Ding, F., Dragutan, I., & Sun, Y. G. La-metal-organic framework incorporating Fe_3O_4 nanoparticles, post-synthetically modified with Schiff base and Pd. A highly active, magnetically recoverable, recyclable catalyst for CC cross-couplings at low Pd loadings. *J. Catal.* **361**, 116–125 (2018).

50. Qi, B., Wu, C., Liu, Y., Liu, J. & Zhang, H. Self-assembled magnetic Pt nanocomposites for the catalytic reduction of nitrophenol. *ACS Appl. Nano Mater.* **2**, 4377–4385 (2019).

51. Viegas-Junior, C., Danuello, A., da Silva Bolzani, V., Barreiro, E. J., & Fraga, C. A. M. Molecular hybridization: A useful tool in the design of new drug prototypes. *Curr. Med. Chem.* **14**, 1829–1852 (2007).

52. Eldehna, W. M., Altoukhy, A., Mahrous, H. & Abdel-Aziz, H. A. Design, synthesis and QSAR study of certain isatin-pyridine hybrids as potential anti-proliferative agents. *Eur. J. Med. Chem.* **90**, 684–694 (2015).

53. Fortin, S. & Bérubé, G. Advances in the development of hybrid anticancer drugs. *Expert Opin. Drug Discov.* **8**, 1029–1047 (2013).

54. Khidre, R. E. & Radini, I. A. M. Design, synthesis and docking studies of novel thiazole derivatives incorporating pyridine moiety and assessment as antimicrobial agents. *Sci. Rep.* **11**, 7846 (2021).

55. Bull, J. A., Mousseau, J. J., Pelletier, G. & Charette, A. B. Synthesis of pyridine and dihydropyridine derivatives by regio-and stereoselective addition to *N*-activated pyridines. *Chem. Rev.* **112**, 2642–2713 (2012).

56. Rashdan, H. R., Shehadi, I. A. & Abdelmonsef, A. H. Synthesis, anticancer evaluation, computer-aided docking studies, and ADMET prediction of 1, 2, 3-triazolyl-pyridine hybrids as human aurora B kinase inhibitors. *ACS Omega* **6**, 1445–1455 (2021).

57. Gygi, D., Hwang, S. J. & Nocera, D. G. Scalable syntheses of 4-substituted pyridine–diimines. *J. Org. Chem.* **82**, 12933–12938 (2017).

58. Torabi, M., Yarie, M., Baghery, S., & Zolfigol, M. A. Recent advances in catalytic synthesis of pyridine derivatives 503–580 (2023).

59. Zafar, R. *et al.* Prospective application of two new pyridine-based Zinc (II) amide carboxylate in management of alzheimer's disease: Synthesis, characterization, computational and in vitro approaches. *Drug Des. Devel. Ther.* **15**, 2679 (2021).

60. Mrozek-Wilczkiewicz, A., Malarz, K., Rejmund, M., Polanski, J. & Musiol, R. Anticancer activity of the thiosemicarbazones that are based on di-2-pyridine ketone and quinoline moiety. *Eur. J. Med. Chem.* **171**, 180–194 (2019).

61. Dawood, D. H. *et al. RSC Adv.* **11**, 29441–29452 (2021).

62. Salar, U. *et al.* Coumarin sulfonates: New alkaline phosphatase inhibitors; in vitro and in silico studies. *Eur. J. Med. Chem.* **131**, 29–47 (2017).

63. Vieira, B. M. *et al.* Ultrasound-assisted synthesis and antioxidant activity of 3-selanyl-1*H*-indole and 3-selanylimidazo [1, 2-*a*] pyridine derivatives. *Asian J. Org. Chem.* **6**, 1635–1646 (2017).

64. Desai, N., Jadeja, D., Mehta, H., Khasiya, A. K., & Shah, U. Pandit, *N*-Heterocycles. Springer, Singapore 143–189 (2022).

65. Alizadeh, S. R. & Ebrahimzadeh, M. A. Antiviral activities of pyridine fused and pyridine containing heterocycles, a review (from 2000 to 2020). *Mini-Rev. Med. Chem.* **21**, 2584–2611 (2021).

66. Mermer, A., Keles, T. & Sirin, Y. *Bioorg. Chem.* **114**, 105076–105124 (2021).

67. Rodríguez, I. *et al.* Apoptosis pathways triggered by a potent antiproliferative hybrid chalcone on human melanoma cells. *Int. J. Mol. Sci.* **22**, 13462 (2021).

68. Toure, B. B. & Hall, D. G. Natural product synthesis using multicomponent reaction strategies. *Chem. l Rev.* **109**, 4439–4486 (2009).

69. MacParland, S. A. *et al.* Single cell RNA sequencing of human liver reveals distinct intrahepatic macrophage populations. *Nat. commun.* **9**, 4383 (2018).

70. Torabi, M. *et al.* Synthesis of new pyridines with sulfonamide moiety via a cooperative vinylogous anomeric-based oxidation mechanism in the presence of a novel quinoline-based dendrimer-like ionic liquid. *RSC Adv.* **11**, 3143–3152 (2021).

71. Karimi, F., Yarie, M. & Zolfigol, M. A. Synthesis and characterization of $Fe_3O_4@SiO_2@(CH_2)_3NH(CH_2)_2O_2P(OH)_2$ and its catalytic application in the synthesis of benzo-[*h*] quinoline-4-carboxylic acids via a cooperative anomeric based oxidation mechanism. *Mol. Catal.* **489**, 110924 (2020).

72. Ghasemi, P., Yarie, M., Zolfigol, M. A., Taherpour, A. A. & Torabi, M. Ionically tagged magnetic nanoparticles with urea linkers: application for preparation of 2-aryl-quinoline-4-carboxylic acids via an anomeric-based oxidation mechanism. *ACS Omega* **5**, 3207–3217 (2020).

73. Karimi, F., Yarie, M. & Zolfigol, M. A. *RSC Adv.* **10**, 25828 (2020).

74. Zarei, N., Torabi, M., Yarie, M. & Zolfigol, M. A. Functionalized hybrid magnetic catalytic systems on micro- and nanoscale utilized in organic synthesis and degradation of dyes. *Polycycl. Aromat. Compd.* **4**, 1263–1307 (2022).

75. Fazl, F., Torabi, M., Yarie, M. & Zolfigol, M. A. Synthesis and application of novel urea–benzoic acid functionalized magnetic nanoparticles for the synthesis of 2,3-disubstituted thiazolidin-4-ones and hexahydroquinolines. *RSC Adv.* **12**, 16342–16353 (2022).

76. Torabi, M., Yarie, M., Zolfigol, M. A., Azizian, S. & Gu, Y. A magnetic porous organic polymer: Catalytic application in the synthesis of hybrid pyridines with indole, triazole and sulfonamide moieties. *RSC Adv.* **12**, 8804–8814 (2022).

77. Yarie, M. Catalytic anomeric based oxidation. *Iran. J. Catal.* **7**, 85–88 (2017).

78. Yarie, M. Spotlight: Catalytic vinylogous anomeric based oxidation (Part I). *Iran. J. Catal.* **10**, 79–83 (2020).

79. Torabi, M., Zolfigol, M. A., Yarie, M. & Gu, Y. Application of ammonium acetate as a dual rule reagent-catalyst in synthesis of new symmetrical terpyridines. *Mol. Catal.* **516**, 110959 (2021).

80. Kalhor, S. *et al.* Synthesis of 2-amino-6-(1*H*-indol-3-yl)-4-phenylnicotinonitriles and bis(indolyl) pyridines using a novel acidic nanomagnetic catalyst via a cooperative vinylogous anomeric-based oxidation mechanism. *Polycycl. Aromat. Compd.* **11**, 4270–4285 (2021).

81. Torabi, M., Zolfigol, M. A., Yarie, M., Notash, B., Azizian, S., & Mirzaei Azandaryani, M. Synthesis of triarylpyridines with sulfonate and sulfonamide moieties via a cooperative vinylogous anomeric-based oxidation. *Sci. Rep.* **11**, 16846 (2021).

82. Dashteh, M. *et al.* A convenient catalytic method for the synthesis of pyridines with henna and pyrazole moieties using cooperative vinylogous anomeric-based oxidation. *Chem. Select* **7**, e202200346 (2022).

83. Alabugin, I. V. *et al.* Stereoelectronic power of oxygen in control of chemical reactivity: the anomeric effect is not alone. *Chem. Soc. Rev.* **50**, 10253–10345 (2021).

84. Alabugin, I. V., Kuhn, L., Krivoshchapov, N. V., Mehaffy, P. & Medvedev, M. G. *Chem. Soc. Rev.* **50**, 10212–10252 (2021).

85. Arlan, F. M., Marjani, A. P., Javahershenas, R. & Khalafy, J. Recent developments in the synthesis of polysubstituted pyridines via multicomponent reactions using nanocatalysts. *New J. Chem.* **45**, 12328–12345 (2021).

86. Akhmadiev, N. S., Akhmetova, V. R. & Ibragimov, A. G. 2-Amino-3, 5-dicarbonitrile-6-sulfanylpyridines: Synthesis and multiple biological activity–a review. *RSC Adv.* **11**, 11549–11567 (2021).

87. Gebre, S. H. Recent developments of supported and magnetic nanocatalysts for organic transformations: an up-to-date. *Appl. Nanosci.* (2021).

88. Asressu, K. H., Chan, C. K. & Wang, C. C. One-pot synthesis of 1, 5-diketones under a transition-metal-free condition: Application in the synthesis of 2, 4, 6-triaryl pyridine derivatives. *ACS Omega* **6**, 7296–7311 (2021).

89. Makoś, P., Fernandes, A., Przyjazny, A. & Boczkaj, G. Sample preparation procedure using extraction and derivatization of carboxylic acids from aqueous samples by means of deep eutectic solvents for gas chromatographic-mass spectrometric analysis. *J. Chromatogr. A.* **1555**, 10–19 (2018).

90. Shafie, M. H., Yusof, R & Gan, C. Y. *J. Mol. Liq.* **288**, 111081–111087 (2019).

91. Figueiredo, M. *et al.* Differential capacity of a deep eutectic solvent based on choline chloride and glycerol on solid electrodes. *Electrochim. Acta.* **54**, 2630–2634 (2009).

92. Ling, J. K. U., San Chan, Y., Nandong, J., Chin, S. F., & Ho, B. K. *Lwt*, **133**, 110096–110106 (2020).

93. Silva, J. M., Reis, R. L., Paiva, A. & Duarte, A. R. C. *ACS Sustain. Chem. Eng.* **6**, 10355–10363 (2018).

94. Subba, N., Sahu, P., Das, N. & Sen, P. Rational design, preparation and characterization of a ternary non-ionic room-temperature deep eutectic solvent derived from urea, acetamide, and sorbitol. *J. Chem. Sci.* **133**, 25 (2021).

Acknowledgements

Author contributions

Competing interests

The authors declare no competing interests.

Additional information

Supplementary Information The online version contains supplementary material available at https://doi.org/10.1038/s41598-023-35849-3.

Correspondence and requests for materials should be addressed to M.A.Z. or M.Y.

Reprints and permissions information is available at www.nature.com/reprints.

Publisher's note Springer Nature remains neutral with regard to jurisdictional claims in published maps and institutional affiliations.